Ecological Applications, 00(0), 0000, pp. 000–000

Assessment of boreal forest historical C dynamics in Yukon River Basin: relative roles of warming and fire regime change

F.-M. Yuan,[1,8] S.-H. Yi,[2] A. D. McGuire,[3] K. D. Johnson,[1,9] J. Liang,[4,10] J. W. Harden,[5] E. S. Kasischke,[6] and W. A. Kurz[7]

[1]*Institute of Arctic Biology, University of Alaska, Fairbanks, Alaska 99775 USA*
[2]*State Key Laboratory of Cryosphere Sciences, Cold and Arid Regions Environmental and Engineering Research Institute, CAS, Lanzhou, Gansu, China*
[3]*U.S. Geological Survey, Alaska Cooperative Fish and Wildlife Research Unit, University of Alaska, Fairbanks, Alaska 99775 USA*
[4]*School of Natural Resources and Agricultural Sciences, University of Alaska, Fairbanks, Alaska 99775 USA*
[5]*U.S. Geological Survey, Menlo Park, California 94025 USA*
[6]*Department of Geographical Sciences, University of Maryland, College Park, Maryland 20741 USA*
[7]*Natural Resources Canada, Canadian Forest Service, Victoria, British Columbia V8Z 1M5 Canada*

Abstract. Carbon (C) dynamics of boreal forest ecosystems have substantial implications for efforts to mitigate the rise of atmospheric CO_2 and may be substantially influenced by warming and changing wildfire regimes. In this study we applied a large-scale ecosystem model that included dynamics of organic soil horizons and soil organic matter characteristics of multiple pools to assess forest C stock changes of the Yukon River Basin (YRB) in Alaska, USA, and Canada from 1960 through 2006, a period characterized by substantial climate warming and increases in wildfire. The model was calibrated for major forests with data from long-term research sites and evaluated using a forest inventory database. The regional assessment indicates that forest vegetation C storage increased by 46 Tg C, but that total soil C storage did not change appreciably during this period. However, further analysis suggests that C has been continuously lost from the mineral soil horizon since warming began in the 1970s, but has increased in the amorphous organic soil horizon. Based on a factorial experiment, soil C stocks would have increased by 158 Tg C if the YRB had not undergone warming and changes in fire regime. The analysis also identified that warming and changes in fire regime were approximately equivalent in their effects on soil C storage, and interactions between these two suggests that the loss of organic horizon thickness associated with increases in wildfire made deeper soil C stocks more vulnerable to loss via decomposition. Subbasin analyses indicate that C stock changes were primarily sensitive to the fraction of burned forest area within each subbasin and that boreal forest ecosystems in the YRB are currently transitioning from being sinks to sources at ~0.7% annual area burned. We conclude that it is important for international mitigation efforts focused on controlling atmospheric CO_2 to consider how climate warming and changes in fire regime may concurrently affect the CO_2 sink strength of boreal forests. It is also important for large-scale biogeochemical and earth system models to include organic soil dynamics in applications to assess regional C dynamics of boreal forests responding to warming and changes in fire regime.

Key words: assessment; basin-scale analysis; boreal forests; climate warming; C stock dynamics; dynamic organic soil; fire regime change; terrestrial ecological modeling.

Introduction

Terrestrial ecosystems act as a key control on climate warming by sequestering a significant portion of anthropogenic CO_2 emissions into natural sinks (Canadell et al. 2007*a*). However, these rates of sequestration are neither permanent nor fixed, and there is evidence suggesting that the efficiency of terrestrial ecosystems to sequester anthropogenic CO_2 emissions may be weakening (Canadell et al. 2007*a*, *b*). The weakening of terrestrial sinks has important implications for international climate policy to manage the global carbon cycle. Efforts to assess the efficiency of terrestrial sinks have largely been conducted at the global scale (Canadell et al. 2007*a*, Le Quere et al. 2009), but it is important that

Manuscript received 31 October 2011; revised 30 May 2012; accepted 31 May 2011. Corresponding Editor: D. S. Schimel.
[8] Present address: Climate Change Science Institute and Environmental Science Division, Oak Ridge National Laboratory, Oak Ridge, Tennessee 37831 USA.
E-mail: yuanf@ornl.gov
[9] Present address: USDA Forest Service, Climate Fire and Carbon Cycle Sciences, Newtown Square, Pennsylvania 19073 USA.
[10] Present address: Division of Forestry and Natural Resources, Davis College of Agriculture, Nature Resources and Design, West Virginia University, Morgantown, West Virginia 26506 USA.

the assessment of the efficiency of sinks incorporate regional details and insights to better understand how and why sink strength is changing to better inform climate policy related to the management of the global carbon cycle (Canadell et al. 2011). Because of the large amount of carbon stored in the boreal forest, there is concern that climate warming and associated increases in fire disturbance could affect the CO_2 sink strength of this region (McGuire et al. 2009, Pan et al. 2011). In this study, we conducted an assessment of historical carbon stock dynamics in the Yukon River Basin (YRB) of Alaska, USA, and Canada to provide insight into how and why sink strength is changing in the region and to understand the potential implications of these dynamics for carbon management policy. In the *Introduction* we review what is generally known about the strength of CO_2 sinks in boreal forests, identify some of the limitations of regional analyses on CO_2 sinks that have been conducted to date, and then provide an overview of our approach to overcome some of these limitations in our assessment of historical carbon stock dynamics of the YRB.

Boreal forest ecosystems have functioned as sinks for atmospheric CO_2 for many millennia, and this has led to the accumulation of substantial soil organic carbon (C) stocks in permafrost and peatlands (Harden et al. 1992, McGuire et al. 2009, Tarnocai et al. 2009). Boreal forests have been estimated to be important sinks for atmospheric CO_2 in the late 20th century and early 21st century (McGuire et al. 2009, Pan et al. 2011). Forest inventory analyses indicate that boreal forests have been responsible for 22% of the residual terrestrial CO_2 sink (after accounting for the effects of tropical deforestation) between 1990 and 2007 (Pan et al. 2011), and it was estimated that 41% of the 496 Tg C/yr increase in boreal forest C storage between 1990 and 2007 occurred in litter and soil C pools. While the estimated changes in boreal forest vegetation C and dead wood biomass by Pan et al. (2011) are reasonably constrained by forest inventory measurements, changes in organic and mineral soil C pools have been based on model estimates in which soil C tends to increase with increasing vegetation C storage. There are concerns that the sink in some boreal regions is weakening and may have become a source due to wildfire and other disturbances (McGuire et al. 2010*a*, Hayes et al. 2011, Stinson et al. 2011, Turetsky et al. 2011). Several regional analyses indicate that permafrost thaw and increases in wildfire associated with climate warming could release substantial amounts of soil C from boreal forests in the future (Zhuang et al. 2006, Balshi et al. 2009, Schaefer et al. 2011, Schneider von Deimling et al. 2012). Such losses have consequences for the global climate system in that they might enhance the rate of climate warming and therefore may compromise efforts to mitigate the rise of CO_2 in the atmosphere. Thus, there is a need to more comprehensively analyze how soil C stocks of boreal forests are responding to climate warming and changes in the fire regime.

One limitation of regional analyses to date is that they have treated soil organic horizons as static with respect to estimating the effects of warming and fire on organic soil horizon thickness and composition, and thus, on soil thermal dynamics and hydrology. Yet, the thickness and composition of soil organic horizons are quite variable in both space and time in Alaska (Barrett et al. 2011, Johnson et al. 2011). Site-specific modeling analyses indicate that the thickness and structure of soil organic horizons have important influences on soil thermal dynamics that affect biogeochemical responses to soil warming and wildfire (Zhuang et al. 2002, Yi et al. 2007, 2009*a*). It is important to consider the dynamics of soil organic horizons because these horizons play a critical role in permafrost stability, as they insulate permafrost from summer air temperature (Yi et al. 2007, O'Donnell et al. 2009*a*, *b*, Jorgenson et al. 2010, Turetsky et al. 2010). Yi et al. (2007) showed that soil organic horizons can protect permafrost from degradation caused by climate warming. However, the removal of soil organic horizons by fire exposes permafrost to thaw by modifying surface energy balance and soil thermal conditions, and in a warming climate, permafrost may undergo long-term thaw from this exposure (Yoshikawa et al. 2003, Yi et al. 2009*b*, 2010). It is therefore important to represent the dynamics of soil organic horizons in assessing how soil C responds to both climate warming and changes in fire regime.

Thus, a key challenge to assessing regional changes in carbon stocks in the boreal forest is to represent how the structure and composition of soil organic horizons response to climate warming and changes in fire regime. In this study we applied a large-scale ecosystem model representing the dynamics of organic soil horizons to estimate changes in forest C stocks of the YRB in Alaska and Canada from 1960 through 2006. The YRB has experienced substantial warming of climate and increases in wildfire extent and severity over this time period (Kasischke and Turetsky 2006, Kasischke et al. 2010, Barrett et al. 2011). Our objective in this study was to use the model as a tool to quantify the relative roles of warming and changes in fire regime on simulated changes in forest vegetation and soil C stocks of the YRB from 1960 to 2006, and consequently, changes to the strength of the boreal forest CO_2 sink in the region. Our analysis is also relevant to whether the tools used in assessments of regional to global carbon dynamics should consider the dynamics of organic soil horizon structure and composition in assessing how C storage of boreal forests respond to ongoing and projected climate warming and changes in fire regime. To our knowledge, this is the first regional application of a model that includes these types of dynamics of organic soil horizons in boreal forests.

Materials and Methods

Overview

In this study we used the dynamic organic soil version of the Terrestrial Ecosystem Model (DOS-TEM; Yi et al. 2009*a*, *b*, 2010) as a tool to understand the relative roles of climate warming and changes in fire regime on the dynamics of forest ecosystem C in the YRB from 1960 to 2006. The DOS-TEM has been designed to explicitly represent the effects of fire on interactions among soil thermal and hydrologic dynamics, the structure of organic soil horizons, and ecosystem biogeochemistry. For this study, we modified the decomposition dynamics of DOS-TEM to represent multiple C pools of different quality within different layers of the organic and mineral soil horizons. We then parameterized and calibrated the DOS-TEM for black spruce, white spruce, and deciduous forest types based on soil C pools from a soil C database for interior Alaska and based on estimates of vegetation biomass C and N pools and fluxes from studies conducted by the Bonanza Creek Long-Term Ecological Research (LTER) forest sites located near Fairbanks, Alaska. The model was then validated by comparing simulated estimates of forest aboveground biomass and soil organic horizon thickness to those of a forest inventory database in Alaska. We then applied the model to analyze changes in forest vegetation and soil C stocks of the YRB from 1960 to 2006, driven by historical climate (monthly from 1900 to 2006) and a historical fire database (from 1960 to 2006; "historical simulation"). We analyzed changes in estimated C stocks of 13 subbasins of the YRB in relation to the amount of warming and fire experienced by each subbasin between 1960 and 2006. To evaluate the relative importance of warming and changes in the fire regime on C stocks of the entire basin over this time period, we conducted a factorial analysis to evaluate the effects of climate warming (historical vs. detrended air temperature) and changes in fire regime (historical vs. normalized fire regime).

Model description and development

Previous versions of the Terrestrial Ecosystem Model (TEM) have been applied to evaluate how historical changes in climate and fire regime influence regional C dynamics of northern high-latitude ecosystems (Balshi et al. 2007, McGuire et al. 2010*b*, Hayes et al. 2011). However, these applications treated soil thermal and hydrologic dynamics based on a static description of the thickness of soil organic horizons and did not represent how the alteration of soil organic horizons by fire influence biogeochemistry through the coupled responses of soil thermal and hydrologic dynamics. In site-specific evaluations of static vs. dynamic implementations of organic soil in TEM, Yi et al. (2010) showed that, without the dynamic linkage between organic soil horizon thickness and C content, the model overestimates soil C in deep mineral soil horizons of dry black spruce ecosystems of interior Alaska. Furthermore, the results of Yi et al. (2010) show that both soil drainage and fire frequency are important in the C dynamics simulated by DOS-TEM, and should be considered in spatial applications of the model. In this study, we describe one of the first regional applications of DOS-TEM that considers spatial variability in soil drainage and both spatial and temporal variability in fire frequency across the YRB to evaluate how climate warming and changes in fire regime influence C cycling in the basin. The development and testing of DOS-TEM at individual sites for black spruce forest have been described by Yi et al. (2009*a*, *b*, 2010). Here we provide a general description of the DOS-TEM model framework, and describe the additional development of the version of DOS-TEM used in this study.

There are four components in DOS-TEM: the environmental module (EnvM), the ecological module (EcoM), the fire effects module (FEM), and the dynamic organic soil module (DOSM) (Fig. 1). The purpose of the EnvM is to provide the EcoM with information on the atmospheric and soil environment and to provide the FEM with information on the soil environment. Specifically, the EnvM calculates the dynamics of biophysical processes driven by data on climate, landscape position, mineral soil texture, leaf area index (from the EcoM), and soil structure (from the DOSM). In the DOSM, a soil column is composed of four types of "horizons" including moss (live surface material), fibrous organic (slightly decomposed fibric organics), amorphous organic (moderately to very decomposed organics with amorphous material), and mineral horizons. Within each horizon, there can be one to several "layers" of prescribed thickness to accurately resolve soil thermal and hydrologic dynamics. The C content of each of the layers within the fibrous, amorphous, and mineral horizons is explicitly tracked in the DOSM.

The EnvM operates at a daily time step driven by daily air temperature, vapor pressure, surface solar radiation, and precipitation, which are interpolated from monthly input data. The EnvM considers the radiation and water fluxes among the atmosphere, canopy, snow pack, and soil. Changes in the thickness of moss and the fibrous and amorphous organic horizons are calculated by the DOSM based on information from the EcoM. Each horizon can have one to multiple layers depending on the thickness of the horizon. Soil moisture and temperature are updated by the EnvM for each layer on a daily basis. A two-directional Stefan algorithm is used to predict the positions of freezing/thawing fronts in the soil. The temperature of soil layers above the top freezing/thawing front and below the bottom freezing/thawing front is updated separately by solving finite difference equations. Temperatures of the soil layers between the first and last freezing/thawing fronts are assumed to be at the freezing point. Soil moisture is only updated for unfrozen layers by solving the Richards' equation. Both the thermal (e.g., thermal conductivity and heat capacity) and hydraulic properties (e.g., hydraulic conductivity) of soil layers are affected by their water content. It is important to recognize that the EnvM only

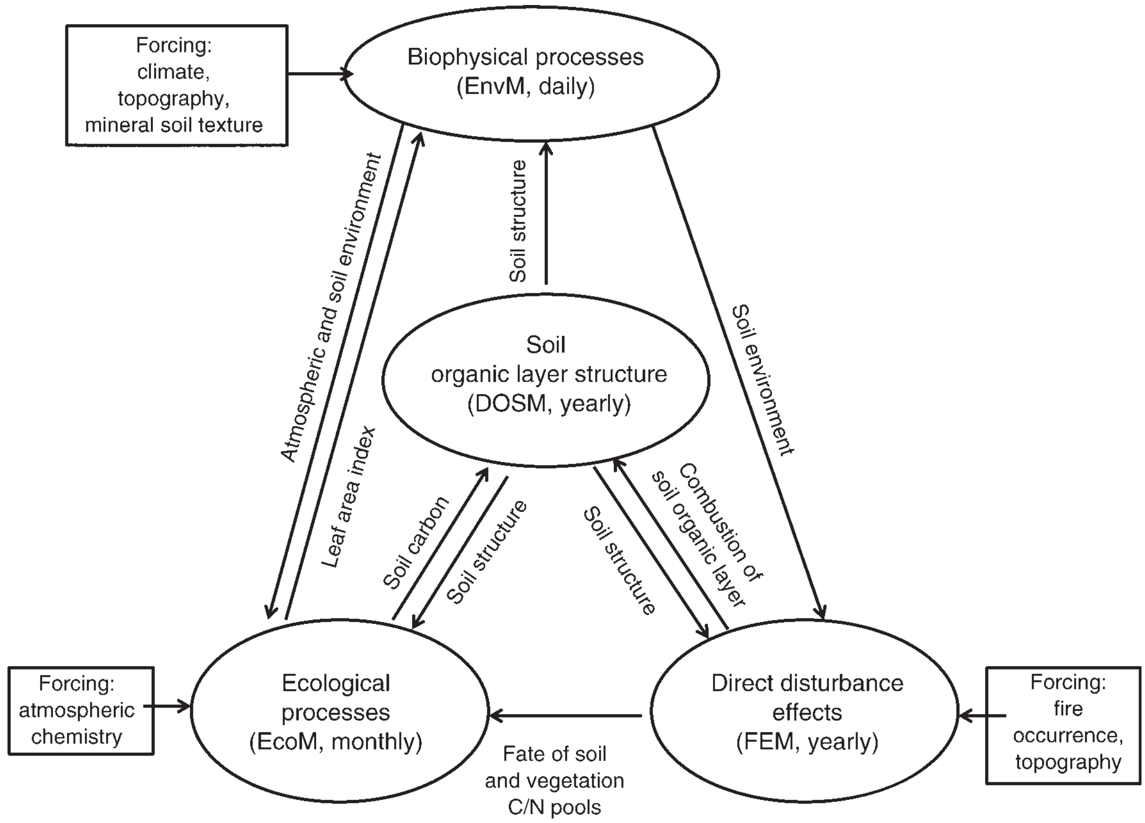

FIG. 1. Interactions among modules of the dynamic organic soil version of the Terrestrial Ecosystem Model (DOS-TEM). Modules include the daily environmental module (EnvM), the monthly ecological module (EcoM), the annual fire effects module (FEM), and the dynamic organic soil module (DOSM). "Forcing" indicates drivers of the modeled processes, i.e., inouts needed to run the model. The arrows show how the data flow between the modules.

models vertical thaw/freeze and does not model subsidence associated with the thawing of ice in soil thermal layer. Thus, the model does not consider the effects of themokarst disturbance that might be associated with thawing permafrost. The simulated estimates of daily evapotranspiration, soil temperature, and moisture are averaged to monthly values, and provided to EcoM. See Yi et al. (2009*b*) for more details on the EnvM and an evaluation of the performance of the soil temperature and moisture simulations by the module.

The EcoM uses information on atmospheric chemistry, atmospheric, and soil environmental conditions calculated by the EnvM, soil structure (from the DOSM), and the effects of disturbance on soil and vegetation C and N pools (from the FEM) to simulate vegetation and soil C and N pools of the ecosystem (Fig. 1). Information on soil C changes is provided to the DOSM yearly so that it can alter the thicknesses of organic soil horizons. In contrast to previous versions of TEM, DOS-TEM (Yi et al. 2010) simulates the dynamics of three different soil horizons (the fibrous, amorphous, and mineral soil horizons). Because the decomposition rates in the model are defined separately for each horizon, this version of TEM is capable of representing multiple soils of different quality that are stratified vertically. The C from litterfall is divided into aboveground litterfall and belowground litterfall (root mortality). Aboveground litterfall is assigned only to the first layer of the fibrous horizon, while belowground litterfall is assigned to different layers of the three horizons based on the fractional distribution of fine roots with depth. The dynamics of coarse woody debris, an important C pool associated with fire disturbance in the boreal forest (Manies et al. 2005), are also considered in DOS-TEM. EcoM was run at a monthly time step. More details on the implementation of EcoM can be found in Yi et al. (2010).

The two primary modifications we made to EcoM in this study involved (1) the representation of multiple soil C pools within each layer of the fibrous, amorphous, and mineral soil horizons in DOSM; and (2) the way in which the normalized foliage growth index is estimated in the EcoM. In the original version of EcoM, soil C was tracked as a single pool for each layer of the fibrous, amorphous, and mineral soil horizons. In this study, we implemented the conceptual model of Jenkinson and Rayner (1977) where litter first decomposes into two C pools, decomposable plant material, and resistant plant material. Because the DOS-TEM calibrates decomposition rates, we classified ground organic materials and soil organic matter (SOM) into four C pools within each layer of the fibrous, amorphous, and mineral horizons: (1) a coarse plant material pool (litter), (2) an active soil C pool (i.e., soil biomass C) with very quick decomposition, (3) a physically resistant soil C pool of moderate decomposition, and (4) a chemically resistant soil C pool of nearly stabilized (very slow decomposition), which also represents the charred C that is retained during fire.

In the model, total litterfall C (C_{ltfl}), i.e., the inputs into the coarse plant material pools, is first calculated as the proportion of total vegetation C in each time step

$$C_{\mathrm{ltfl}} = \mathrm{CFALL_v} \times C_{\mathrm{v}} \tag{1}$$

where $\mathrm{CFALL_v}$ is a vegetation-specific parameter. Total litterfall C then is partitioned into above- and belowground components based on the vegetation-specific aboveground to belowground ratio. Aboveground plant litterfall is input into the coarse plant material C pool within the top layer of the fibrous horizon, and belowground plant litterfall (root turnover or mortality due to fire) is input into those coarse-plant material C pools in their rooted layers according to a prescribed root fraction distribution with depth prescribed from observations.

Decomposition of C in the plant material pool and the further decomposition of three resultant SOM component pools (i.e., active, physically and chemically resistant pools) results in the transfer of 7.6% of that C into the active C pool, 12.5% into the physically resistant C pool, 0.35% into the chemically resistant C pool, and the remainder is released as CO_2 into the atmosphere (Jenkinson and Rayner 1977). Based on these percentages, 0.0955, 0.1571, and 0.0044 g C of active, physically resistant, and chemically resistant SOM, respectively, would be formed, if 1 g C of CO_2 is respired into the atmosphere, or, the ratio of total SOM-C to CO_2-C production is 0.2570 in soil C decomposition.

In DOS-TEM, therefore, the release of CO_2 into the atmosphere is first calculated as the heterotrophic respiration (R_{H}) from each layer for each C pool as described by Yi et al. (2010) as follows:

$$R_{\mathrm{H}j,i} = K_{\mathrm{D}j,i} C_{\mathrm{S}j,i} f(M_{\mathrm{v},i}) f(T_{\mathrm{S},i}) \tag{2}$$

where i is the soil horizon index and j is one of the four soil organic material pools (i.e., coarse plant material and the three SOM components), K_{D} is the respiration rate at 0°C (month^{-1}), C_{S} is the soil C stocks (g C/m^2), and $f(\mathrm{M_v})$ and $f(\mathrm{T_s})$ are the soil moisture and temperature factors, respectively.

Then, from litterfall (Eq. 1) and CO_2 heterotrophic respiration (Eq. 2), the change of the coarse plant material C can be estimated for the surface layer ($C_{\mathrm{SL},0}$ in Eq. 3a), and multiple belowground soil layers ($\mathrm{C_{SL,i}}$ for the ith layer in Eq. 3b) as follows:

$$\Delta C_{\mathrm{SL},0} = C_{\mathrm{ltfl}} F_{\mathrm{above}} + C_{\mathrm{ltfl}} F_{\mathrm{below}} F_{\mathrm{root},0} - R_{\mathrm{HL},0}(1 + r_{\mathrm{tsom}}) \tag{3a}$$

$$\Delta C_{\mathrm{SL},i} = C_{\mathrm{ltfl}} F_{\mathrm{below}} F_{\mathrm{root},i} - R_{\mathrm{HL},i}(1 + r_{\mathrm{tsom}}) \tag{3b}$$

where C_{ltfl} is the total litterfall C (g C/month) from Eq. 1; F_{above} and F_{below} are the litterfall fractions of aboveground vegetation and belowground roots, respectively; F_{root} is the root distribution fraction for each layer of the soils; $R_{\mathrm{HL},i}$ is the coarse plant material CO_2 respiration rate (Eq. 2) in the ith layer (with 0 indicating the surface layer receives aboveground litterfall); and r_{tsom} is the ratio of total SOM production to CO_2 respired (i.e., 0.2570 in this study).

For the three SOM C components ($C_{\mathrm{S}j,i}$ for the jth pool in the ith layer; Eq. 4), the transformation associated with CO_2 respiration from all four C pools will add to each SOM C pool, so their changes can be estimated as

$$\Delta C_{\mathrm{S}j,i} = R_{\mathrm{H}t,i} r_{\mathrm{jsom}} - R_{\mathrm{H}j,i}(1 + r_{\mathrm{tsom}}) \tag{4}$$

where $R_{\mathrm{H}t,i}$ and $R_{\mathrm{H}j,i}$ are total and the jth soil C pools CO_2 respiration in the ith soil layer; and r_{tsom} is the ratio of total SOM production to CO_2 respired (i.e., 0.2570) and r_{jsom} is the ratio of the jth SOM pool production to CO_2 respired (i.e., 0.0955, 0.1571, and 0.0044 for active, physically resistant, and chemically resistant SOM, respectively).

To properly represent the vertical distribution of SOM, a portion of soil organic matter in the model is assumed to be transferred among the three types of horizons: fibrous, amorphous, and mineral. As a simplification of the relevant processes, the model assumes that all three SOM pools from coarse plant material decomposition in the fibrous horizon would be deposited into the underlying amorphous horizon. The fibrous horizon therefore remains relatively coarse textured as it accumulates, and the amorphous horizon contains mostly humified products, in which root mortality is the only source of coarse plant materials. Similarly, a portion (arbitrarily set to 7.5% in this study) of the SOM products from decomposition in the amorphous horizon are transported down and mixed into the top 25 cm mineral horizon. In this way, the mineral horizon accumulates SOM not only through root mortality, but also through the transfer of humified material from the amorphous horizon.

In the EcoM, the calculation of gross primary production (GPP) depends in part on the canopy leaf biomass (C_{vL}) growth scalar and the normalized foliage growth index, f(FOLIAGE), in which C_{vL} is normalized to a theoretical maximal possible leaf biomass (C_{vLmax}) for each vegetation type. The calculation of f(FOLIAGE) is critical to determining the increase in vegetation C after fire disturbance. In previous versions of TEM, this function was represented as a simple hyperbolic relationship with vegetation C. Because a more realistic relationship between canopy leaf biomass and vegetation is described by a sigmoid function, we changed the shape of this relationship so that the normalized index depends on a logistic relationship with vegetation C as described by Zhuang et al. (2002):

$$f(\text{FOLIAGE}) = \frac{1.0}{1.0 + m_1 e^{m_2 \cdot \sqrt{f(C_v)}}} \tag{5a}$$

where, m_1 and m_2 are empirical parameters, and $f(C_v)$ is hyperbolic function of total vegetation C (C_v)

$$f(C_v) = \frac{m_3 C_v}{1.0 + m_4 C_v} \tag{5b}$$

where m_3 and m_4 are empirical vegetation-specific parameters.

The FEM simulates how fire affects C and N pools of vegetation and soil, including combustion emissions to the atmosphere, the fate of uncombusted C and N (live biomass transferred to dead organic matter pools), and the flux of N from the atmosphere to the soil via biological N fixation or deposition in the years following a fire. The amount of soil C combusted is determined by comparing the distribution of soil C with depth to the depth of burn estimated by the FEM. The depth of burning in the organic horizons is based on an index of burn severity ranging from 0 to 1 that depends on the fire season (e.g., early vs. late summer), fire size year (percentage of area burned in interior Alaska), and soil drainage type based on Turetsky et al. (2011) (see Yi et al. 2010 for details). At the time of fire, aboveground vegetation is divided into three parts: live vegetation (1% of prefire aboveground vegetation assumed), combusted vegetation based on French et al. (2002), and uncombusted vegetation. The belowground vegetation was divided into three parts: live roots (1% of prefire roots), uncombusted dead root C, and combusted roots. The amount of uncombusted and combusted roots were determined by comparing the prefire root with the depth of burning into the organic soil horizons. The C in the moss layer was assumed to be completely combusted. N generally follows the fate of C based on C:N ratios of vegetation and soil with the exception that some volatilized N is retained by the ecosystem (a fraction of about 0.3 according to Harden et al. 2004). The net amount of N lost from the ecosystem as a result of fire is reintroduced into the system from the atmosphere annually after a fire in equal annual amounts determined by dividing the total net N lost to the atmosphere during the most recent fire event by fire return interval (FRI). The FEM is implemented once annually if a fire is prescribed.

The DOSM recalculates soil organic thickness after soil C pools are altered by ecological processes and fire disturbance based on the relationships between soil C content and soil organic thickness of different types of organic horizons in black spruce stands (Yi et al. 2009*a*). Based on an analysis of soil organic C in Alaska (Johnson et al. 2011), these relationships are appropriate for white spruce and deciduous forests in Alaska. Once the thickness of each organic soil horizon (i.e., fibrous and amorphous) is determined, DOSM calculates the number of layers in each organic horizon and the thickness of each layer to maintain stability and efficiency of soil temperature and moisture calculations. When fire occurs, the unburned fibrous organic horizon is transferred to the amorphous organic horizon, following Harden et al. (2000), and a 2-cm fibrous organic layer is immediately added on top of amorphous organic layer. In this way, the fibrous organic horizon can start accumulating litterfall and grow.

Model parameterization

We parameterized and calibrated DOS-TEM for three major forest types of the YRB (Yarie and Billings 2002, Calef et al. 2005) in upland and lowland landscape positions: (1) black spruce (*Picea mariana* (Mill.) BSP), (2) white spruce (*Picea glauca* (Moench) Voss), and (3) broadleaf deciduous forests consisting of either quaking aspen (*Populus tremuloides* Michx.), paper birch (*Betula papyrifera* March.), or balsam poplar (*Populus balsamifera* L.).

The parameters for the *f*(FOLIAGE) calculation were based on data sets of forest age sequence stand-level measurements that characterize the vegetation C growth curves for black spruce (Bond-Lamberty and Gower 2007), white spruce (Yarie and Van Cleve 1983), and quaking aspen (for broadleaf deciduous forest; Wang 1995) (Fig. 2a). Because the data for differentiating vegetation growth patterns into upland and lowland stands only exists for black spruce, we did not develop separate sets of parameters for *f*(FOLIAGE) for upland and lowland white spruce and deciduous forests. To translate the growth curves of Fig. 2a into the dependency of normalized foliage growth on stand age (Fig. 2b), we assumed that (1) maximum foliage biomass occurs when the maximum growth rate is achieved, and (2) foliage biomass is exponentially related to vegetation C prior to canopy closure, after which foliage biomass remains at its maximum. The normalized foliage growth index in Fig. 2b was then directly related to vegetation C in Fig. 2a to determine the parameters in the *f*(FOLIAGE) calculation.

We then calibrated the rate-limiting parameters in the EcoM of DOS-TEM based on a soil C data set for interior Alaska and studies of vegetation C and N pools and fluxes by the Bonanza Creek LTER program. We identified the target values of soil C for each of the three forest types in the two landscape positions as the mean soil C plus one standard deviation (SD) from a soil C database compiled for interior Alaska (Table 1; Johnson et al. 2011; National Soil Carbon Network [NSCN], data *available online*).[11] For the target values of vegetation C and N pools and fluxes, we adopted the

[11] http://www.fluxdata.org/nscn/SitePages/Home.aspx

estimates for lowland black spruce, upland and lowland white spruce, lowland balsam poplar, and upland birch-–aspen reported by Ruess et al. (1996) (Table 1). The target values of vegetation C and N pools and fluxes for upland black spruce were based on the estimates from Vogel et al. (2005).

Model validation using the Cooperative Alaska Forest Inventory database

We ran the DOS-TEM at 119 of 191 survey sites, each of which contains three permanent sample plots (PSPs), in the Cooperative Alaska Forest Inventory (CAFI) database (Malone et al. 2009). The 119 sites were those in which the dominant tree species in each site was responsible for >75% of the basal area (Table 2). The climatic variables for those sites were extracted from a $0.5° \times 0.5°$ climate database for the YRB region. Historical fire occurrence was estimated from a 1×1 km fire database for the region that started in the early 1950s (Kasischke et al. 2002, Balshi et al. 2007), and this database was also used to estimate the stand age for each of the sites. The initial soil organic content in 1900 of each site was obtained by an equilibrium simulation in year 1000 using the mean 1901–1930 climate followed by a 900-year spin-up simulation that repeated the 1901–1930 climate 30 times and burned the sites at regular intervals prior to 1900. The model was then run with the historical climate from 1901 to 2006 and burned during that time to reproduce the estimated stand age. The simulated soil organic layer thicknesses in 2006 were compared to the measurements from the CAFI database for 106 of the 119 sites (16 for black spruce, 34 for white spruce, and 56 for deciduous species). For vegetation aboveground biomass, the comparison was conducted between the simulation and forest standing biomass C estimation derived from the CAFI's diameter at breast height (dbh) and tree density according to the allometric equations developed by Yarie et al. (2007).

Model application for boreal forests in Yukon River Basin (YRB) from 1960 to 2006

After validating DOS-TEM, we then applied the model to estimate changes in boreal forest vegetation and soil C storage for the entire YRB. The YRB has an area of 856 385 km^2, and contains 13 subbasins (Table 3). We used the vegetation database developed by Calef et al. (2005) in our model application. The forested area of the basin is 422 794 km^2 (about 49%), and non-forest vegetated area (including upland tundra) occupies 391 480 km^2 (46%) of the basin. The remaining 5% of the basin is barren land and water bodies. About 71% of the forested area is distributed in the seven lower and mid-YRB subbasins that primarily occur within Alaska. About half of the forested area of the YRB is black spruce, and white spruce and deciduous forest species each occupy ~25% of the forested areas of YRB (Table 3). Based on the USGS Compound Topographic Index (CTI) database (1×1 km; *available online*), we estimated

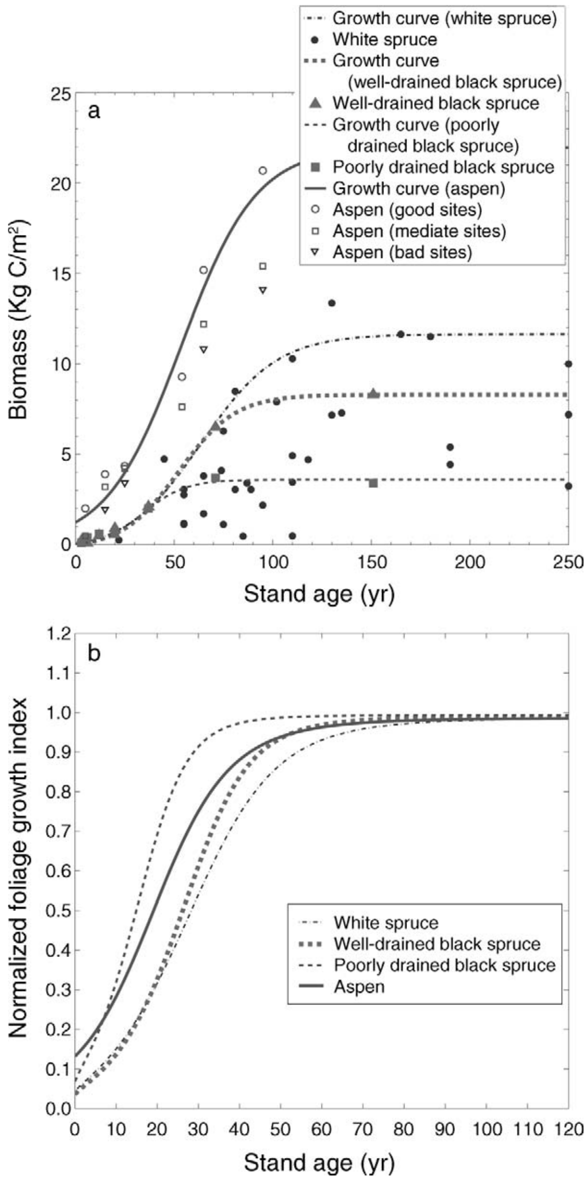

FIG. 2. (a) The biomass growth curves for the major forest types in this study used to derive the (b) foliage growth index in DOS-TEM. Data sources are: black spruce from Manitoba, Canada (Bond-Lamberty and Gower 2007); white spruce in interior Alaska (Yarie and Van Cleve 1983); and aspen in Dawson Creek, British Columbia, Canada (Wang 1995).

that ~41% of the forested area (22.5%, 7.9%, and 10.9% for black spruce, white spruce, and deciduous forests, respectively) in the YRB are located in wet lowlands (CTI $\geq$ 5), while 59% of the forested area (28.0%, 16.9%, and 13.7% for black spruce, white spruce and deciduous trees, respectively) occupy dry uplands (CTI < 5).[12]

In this study, historical data on wildfires in the Alaska part of the YRB are available since the early 1950s, and

[12] http://eros.usgs.gov/#/Find_Data/Products_and_Data_Available/gtopo30/hydro/namerica

TABLE 1. Site target values for C and N state and flux variables used to calibrate the dynamic organic soil version of the Terrestrial Ecosystem Model (DOS-TEM) for major forest types studied in the Yukon River Basin in Alaska, USA, and Canada.

Forest type	Vegetation C (g/m^2)	Vegetation N (g/m^2)	GPP (g·m^{-2}·yr^{-1})	NPP (g·m^{-2}·yr^{-1})	NPP without N limit (g·m^{-2}·yr^{-1})	N uptake (g·m^{-2}·yr^{-1})	Soil C (g/m^2) Total	Soil C (g/m^2) Fibrous layers
Black spruce								
Upland	6405	26.7	372	186	279	1.14	29 300	310
Lowland	2780	13.6	300	152	225	0.92	64 100	3540
White spruce								
Upland	9000	30.5	720	305	458	1.69	10 800	1250
Lowland	8916	30.5	614	307	461	1.35	21 300	1100
Deciduous								
Upland	8546	40.5	1172	510	845	5.25	18 000	1852
Lowland	7758	43.9	1086	543	814	2.23	16 000	2170

Note: The data source for vegetation data is the Bonanza Creek Long-Term Ecological Research forest site, Alaska, USA (Ruess et al. 1996, Vogel et al. 2005), and the data source for soils is the Alaska Soil Organic C Database (Johnson et al. 2011). Abbreviations are: GPP, gross primary productivity; and NPP, net primary productivity.

those for the Canada part of the YRB are available since 1960. Therefore, we focused on the time period from 1960 through 2006. During this analysis period (1960–2006), the mean annual air temperature over the YRB increased by 0.047°C per year, i.e., about 0.5°C per decade, while precipitation did not change appreciably (Fig. 3), based on the extended Climate Research Unit (CRU) data sets described in McGuire et al. (2010*a*) and Hayes et al. (2011). Across the 13 subbasins in the YRB, warming trends for 1960–2006 varied from +0.044°C to +0.056°C per year (Table 3).

Fire frequency between 1960 and 2006 varied substantially across the 13 subbasins of the YRB, ranging from essentially no fire in two upstream basins (Teslin River and Yukon Headwaters basins) to about half of the area burned in the Koyukuk River and Eastern Central Yukon River basins (Table 3). Over the entire YRB, there were three major episodes of fire that occurred in 1969, around 1990, and in 2004–2005 (Fig. 4). The area that burned annually between 1990 and 2006 (17.9% YRB burned in this time period, or 1.1% per year) was nearly three times greater than between 1960 and 1989 (12.2% YRB burned in this time period, or 0.4% per year). In this study, we treated the distribution of fire between 1960 and 1989 as the normalized fire regime and estimated a baseline fire return interval (FRI) for each 0.5° × 0.5° grid cell in the basin using the approach described by Balshi et al. (2007). This FRI database was used to specify fire occurrences throughout the YRB from year 1000 until the first fires identified by the historical databases of fire in Alaska and Canada.

The general procedure for an application of DOS-TEM to each 1 × 1 km grid cell of the YRB involved three continuous stages: a dynamic equilibrium simulation in year 1000, which was then followed by a 900-year spin-up simulation from 1001 to 1900, and a transient simulation from 1901 to 2006 (Yi et al. 2010). The dynamic equilibrium simulations were conducted for all combinations of vegetation types and landscape positions within each 0.5° × 0.5° grid covering the whole YRB, using mean monthly climate drivers of solar radiation, air temperature, precipitation, and air vapor pressure which were averaged between 1901 and 1930 from the historical climate data set described by McGuire et al. (2010*a*) and Hayes et al. (2011). The 900-year spin-up simulations from year 1001 to 1900 were driven by 1901–1930 historical climate data repeatedly for each 1 × 1 km cell of the YRB; the 1 × 1 km resolution of the climate data were generated by a

TABLE 2. Characteristics of the sites (mean ± SD), each of which contains three permanent sample plots (PSPs), of the Cooperative Alaska Forest Inventory (CAFI) database used to evaluate DOS-TEM in this study.

Vegetation type	No. PSPs	Aboveground biomass (g C/m^2)	Soil organic thickness (cm)
Black spruce (>75%)	23	1693 ± 1337	21.4 ± 18.9
White spruce (>75%)	36	3990 ± 2672	14.3 ± 5.9
Deciduous (>75%)	60	5410 ± 1761	10.9 ± 5.2
White spruce – deciduous	26†	5200 ± 1880	10.2 ± 4.5
Deciduous – white spruce	32†	4860 ± 1795	9.6 ± 4.4
Other	4†	. . .	. . .

Note: Ellipses (. . .) indicate that data was not processed.
† Plots not used to verify the model.

Table 1. Extended.

Soil C (g/m^2) Amorphous layers	Mineral layers	Soil total N (g/m^2)	Soil available N (g/m^2)
11 290	17 700	548	0.75
9 560	51 000	671	0.50
1 050	8 500	460	1.50
4 300	15 900	865	1.00
3 448	12 700	679	3.50
930	13 000	784	1.50

simple resampling from the 0.5° × 0.5° historical climate data set. The 1 × 1 km transient simulations from year 1901 to 2006 were driven by the resampled historical climate data.

Fire occurrences applied for 20 fire cycles during the dynamic equilibrium simulations were based on the FRI data set; if FRI exceeded 1000 years, it was set to 1000 years. For the spin-up and transient simulations prior to the start of fires in the historical fire database, fire occurrences were backcasted using the same FRI data sets, but were geographically smoothed and then randomly staggered over time. Fires in the historical fire database were implemented in the latter part of the transient simulations.

The application of DOS-TEM to the YRB for the time period 1960–2006 is referred to as the "historical simulation." In order to analyze the relative importance of warming and fire regime change on C stock changes, we conducted a factorial model simulation experiment as follows: (1) the "+Warming and +Fire" simulation, which is the "historical simulation" as driven by historical climate (from 1901–2006) and observed fire regime (1960–2006); (2) the "−Warming and +Fire" simulation driven by detrended air temperature and observed fire regime; (3) the "+Warming and −Fire" simulation driven by historical climate warming and a normalized fire regime beginning in 1960; and (4) the "−Warming and −Fire" simulation driven by detrended air temperature and normalized fire regime.

The detrended air temperature data set used in simulations 2 and 4 in the paragraph above was generated by detrending monthly air temperature between 1960 and 2006 for each 0.5° × 0.5° grid cell; see Fig. 3a for the comparison between the observed and detrended air temperature data of the YRB. The differences between simulations 1 and 2 or between 3 and 4 were used to estimate the effects of warming.

The normalized fire regime data set used in simulations 3 and 4 was generated by using the FRI data set, which was developed from the 1960–1989 fire data, to extend the backcasted fire data set into the 1960–2006 time period. The forest area burned over the YRB between 1960 and 1989 was comparable between the normalized fire data set (55 600 km^2) and the historical fire data sets (57 900 km^2) (Fig. 4). However, the forest area burned over the YRB between 1990 and 2006 in this normalized fire regime data set (337 000 km^2) was only about half of the area burned in the historical fire data sets (692 000 km^2) for that time period. Therefore, comparisons between simulations 1 and 3or between 2 and 4 allowed us to estimate the effects of changes in fire regime since 1990.

Table 3. Percentage of forested areas, percentage of forested area burned from 1960 to 2006, and mean annual air temperature warming from 1960 to 2006 in the 13 subbasins of Yukon River Basin (YRB).

Subbasins	Forested area: Total (%)	Black spruce (%)	White spruce (%)	Deciduous (%)	Mean annual burned area (%)	Mean air temperature change (°C/yr)
Low and middle Yukon River subbasins						
Lower Yukon River	9.65	4.00	0.66	4.98	0.54	+0.044
West Central Yukon River	10.97	5.29	1.33	4.34	0.72	+0.050
Koyukuk River	9.14	6.01	1.22	1.81	1.04	+0.050
Tanana River	16.9	8.54	2.46	5.91	0.65	+0.050
East Central Yukon River	10.41	6.58	1.86	1.97	1.11	+0.052
Porcupine River	11.56	4.57	3.99	3.00	0.58	+0.056
Chandalar River	2.58	1.60	0.92	0.05	0.78	+0.051
Upper Yukon River subbasins						
Upper Yukon River	7.74	3.21	3.75	0.78	0.38	+0.054
Stewart River	5.12	2.72	2.04	0.35	0.22	+0.056
White River	3.63	1.96	1.55	0.12	0.31	+0.045
Pelly River	5.92	2.58	2.61	0.72	0.05	+0.055
Teslin River	3.68	2.16	1.26	0.26	trace	+0.047
Yukon Headwaters	2.62	1.23	1.06	0.33	trace	+0.053
Total	100.0	50.45	24.82	24.63	0.59	+0.047

Note: Low and middle Yukon River Basins are located mostly in Alaska, USA, and upper Yukon River Basins are mostly in Canada.

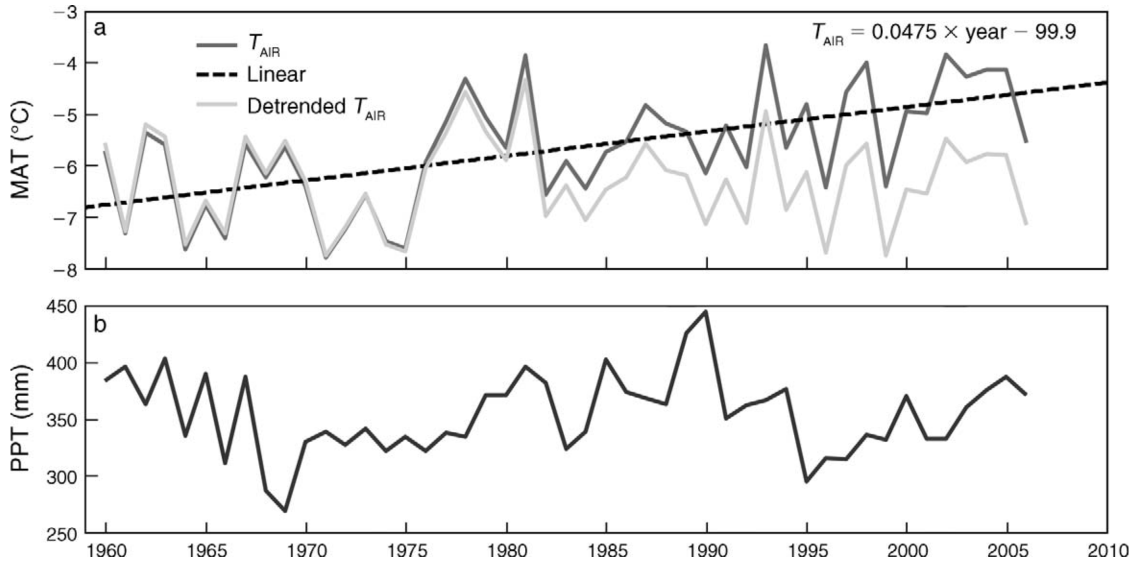

FIG. 3. (a) Mean annual air temperature (MAT, T_{AIR}) and its warming trend, and (b) annual precipitation (PPT) averaged over the Yukon River Basin in Alaska, USA, and Canada, from 1960 to 2006.

RESULTS

Model evaluation

The TEM simulation of aboveground biomass spanned the range of observed aboveground biomass at the CAFI sites (Fig. 5a), even though stand age was estimated from the large-scale fire database assembled for regional simulations. Simulated aboveground biomass was unbiased for black spruce stands (slope = 0.98, $n = 23$, $P = 0.758$ for difference from 1:1 line), slightly overestimated for white spruce stands (slope = 1.07, $n = 36$, $P = 0.01$ for difference from 1:1 line), and significantly underestimated for deciduous forest stands (slope = 0.83, $n = 60$, $P < 0.0001$ for difference from 1:1 line). Simulated and observed aboveground biomass were best correlated for black spruce stands ($R^2 = 0.52$, $n = 23$, $P = 0.0001$), and less well correlated for white spruce ($R^2 = 0.27$, $n = 36$, $P = 0.01$), and not significantly correlated for deciduous forest stands ($R^2 = 0.22$, $n = 60$, $P = 0.11$). Given the substantial uncertainties concerning stand age of the CAFI sites and biomass estimation from allometric equations, these results indicate that the model is generally able to simulate aboveground biomass without much overall bias across spatial

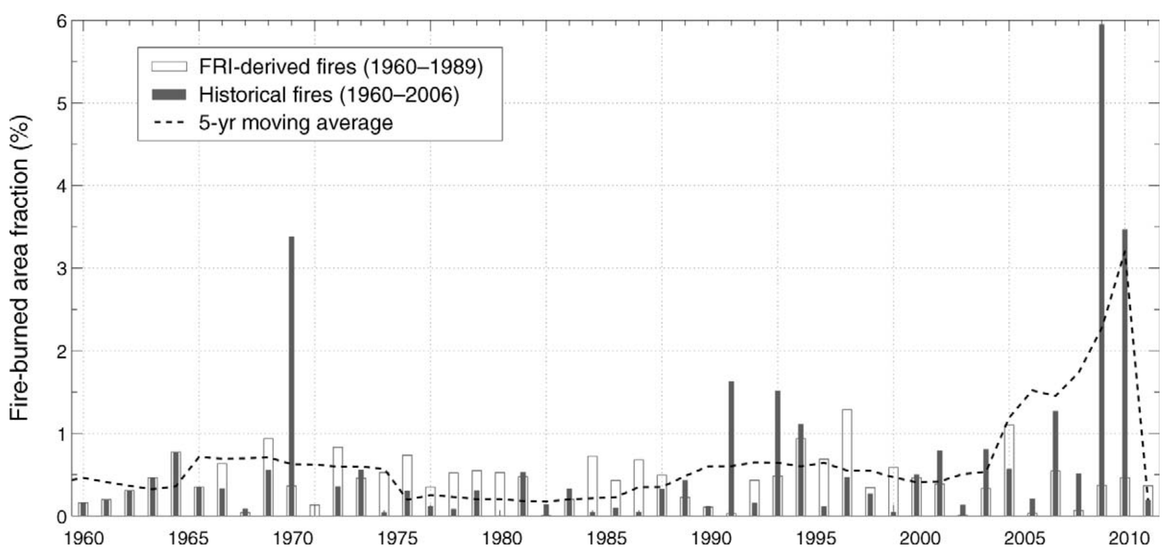

FIG. 4. Percentage of the annual burned area for the time period 1960–2006 vs. the normalized fire regime, based on fire return interval (FRI) derived from fire occurrences from 1960 to 1989) over the forested area of the Yukon River Basin.

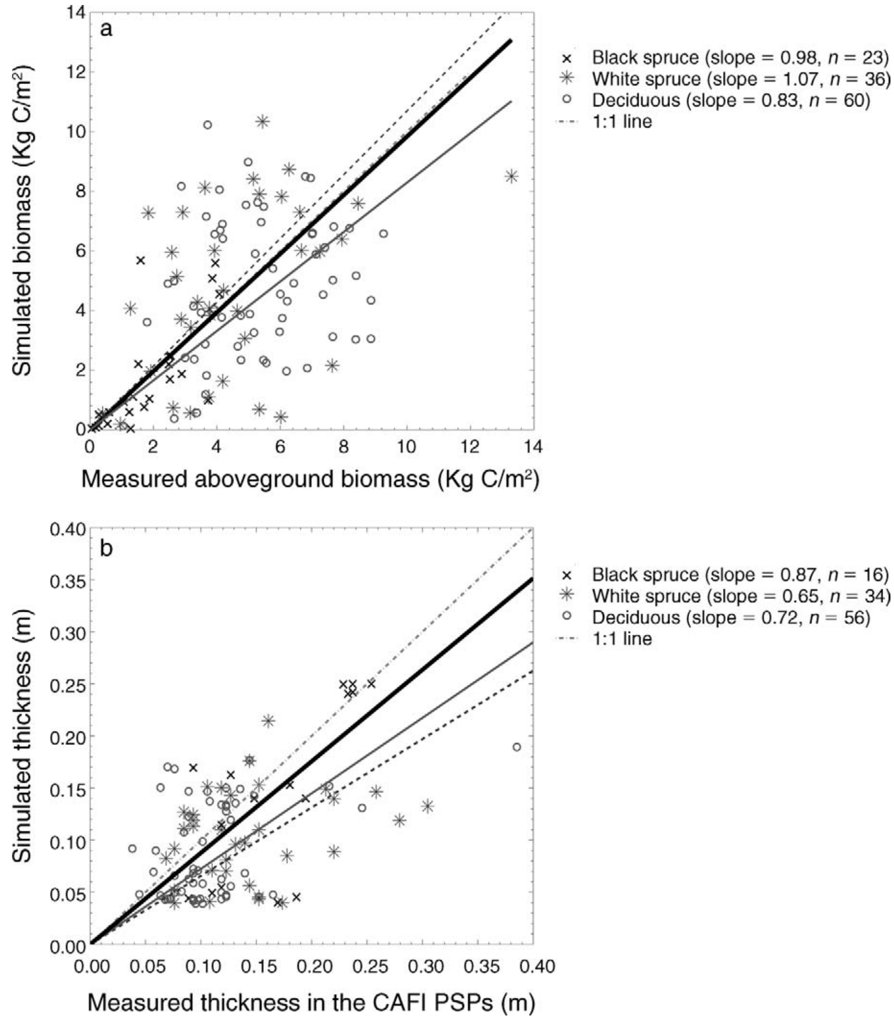

FIG. 5. Comparison of the dynamic organic soil version of the Terrestrial Ecosystem Model (DOS-TEM) estimates with measurements from the Cooperative Alaska Forest Inventory (CAFI) permanent study plots (PSPs): (a) aboveground forest biomass C, and (b) soil organic layer thickness. The lines in the graphs represent the 1:1 line and the regressions lines for black spruce (thick black line), white spruce (gray dashed line), and deciduous species (thin gray line).

domain of the CAFI sites, but it performs better for conifer than for deciduous sites.

The comparison between the TEM estimates and observed soil organic horizon thickness at the CAFI sites showed more scatter than the corresponding analysis for aboveground biomass (Fig. 5b). The model significantly underestimated organic horizon thickness for black spruce stands (slope = 0.87, $n = 16$, $P < 0.0001$ for difference from 1:1 line), white spruce stands (slope = 0.66, $n = 34$, $P < 0.0001$ for difference from 1:1 line), and deciduous forest stands (slope = 0.72, $n = 56$, $P < 0.0001$ for difference from 1:1 line). Simulated and observed thicknesses were best correlated for black spruces stands ($R^2 = 0.52$, $n = 16$, $P = 0.0016$), less well correlated for deciduous forest stands ($R^2 = 0.16$, $n = 56$, $P = 0.002$), and were not significantly correlated for white spruce stands ($R^2 = 0.07$, $n = 34$, P = 0.13). However, the spread of data points in Fig. 5b shows two separate sets of points emanating from the origin of graph: a set of points slightly above the 1:1 line, and a set of points substantially below the 1:1 line. The simulation of horizon thickness slightly overestimates the measured thickness for the set of points above the 1:1 line (slope = 1.09, $R^2 = 0.41$, $n = 100$, $P = 0.001$ for difference from 1:1 line). For the set of points substantially below the 1:1 line, the simulated thickness is very well correlated with measured thickness, but underestimates the thickness by 55% ($R^2 = 0.87$, slope = 0.45, $n = 70$, $P = 0.0003$ for difference from 1:1 line). The underestimation of soil organic horizon thickness at nearly 40% of the CAFI sites are likely associated with uncertainties in representing drainage condition, stand age, the legacies of fire history at the plot scale, inaccurate driving climate data for simulations at the sites, and factors not considered in

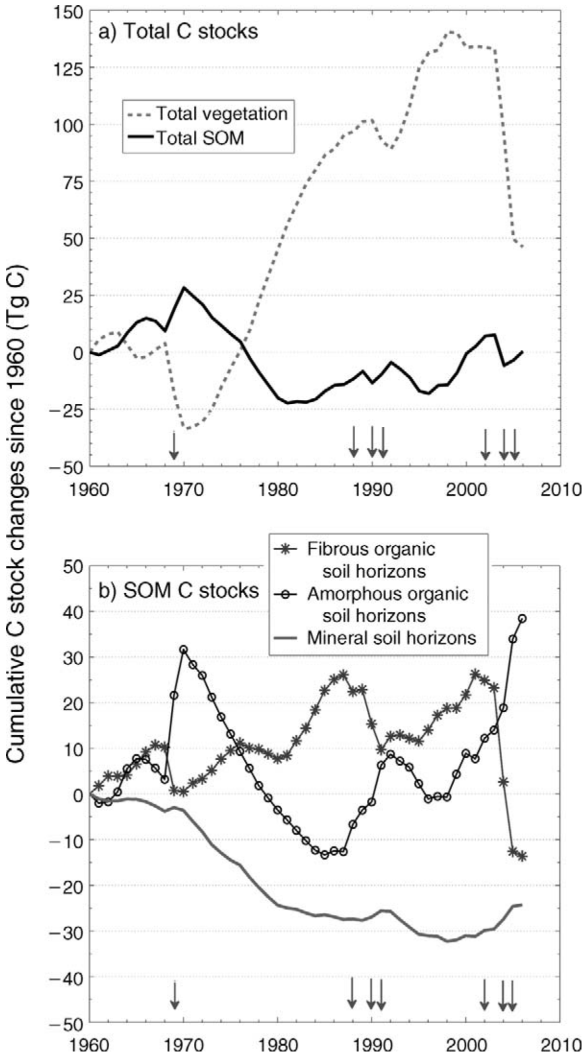

FIG. 6. Cumulative changes in forest C stocks simulated by DOS-TEM for (a) vegetation biomass and total soil organic matter (SOM) and (b) SOM in different soil horizons from 1960 to 2006. Note that the large-fire years (indicated with arrows) are those with a burned area of >1% (see Fig. 4).

the current version of DOSTEM (e.g., the effects of slope and aspect).

Forest C dynamics from 1960 to 2006

From 1960 to the mid-1970s, the YRB experienced a cold period, which was followed by three decades of warming (Fig. 3), a pattern that generally occurred throughout northern high-latitude regions (Euskirchen et al. 2007). In addition, there were three periods of high fire activity that occurred between 1960 and 2006 (Fig. 4): in 1969, from 1988 to 1991, and in 2004 and 2005. The model estimates that total forest vegetation C varied little before 1969 during the cold period, and decreased in response to the large-fire year in 1969 (Fig. 6a). Forest vegetation C quickly recovered after the 1969 fire and increased above 1960 baseline in parallel with increasing temperatures until around 1990, when it decreased in response to the second period of large-fire activity. Again, forest vegetation C quickly recovered and remained relatively stable until it decreased substantially in response to the recent large fires in 2004 and 2005. Over the entire period from 1960 to 2006, DOS-TEM estimates that forest vegetation C increased 46.2 Tg C (2.3 g $C\cdot m^{-2}\cdot yr^{-1}$).

Total soil organic matter (SOM) in the YRB (Fig. 6a) increased slightly in the first half of 1960s during the cold period and even in the fire year of 1969 as organic matter was inherited from substantial input of dead vegetation biomass into the soil. This was followed by several years of SOM loss through the 1980s. SOM increased over both periods of burning (1988–1991 and 2004–2005) and forest regeneration. Over the entire period from 1960 to 2006, DOS-TEM estimated that total forest SOM only increased by 0.4 Tg C.

Although DOS-TEM estimates of total SOM C stocks from the 1960–2006 period did not show significant changes, the model estimated substantial changes in the C content of different soil organic horizons (Fig. 6b). The fibrous SOM horizon increased in the early 1960s because simulated near-surface inputs (via moss and other litterfall) into this horizon were greater than simulated decomposition losses during this cold period. The large fires that occurred around 1969 and 1990 caused an immediate loss via combustion of C in this horizon followed by gains until the next large-fire period. Between 1960 and 2006, the simulation estimates that the fibrous horizon of the YRB lost 14 Tg C, which represents ~2.6% of the 1960 fibrous horizon C, and mostly occurred during the large fires of 2004 and 2005. In contrast to the fibrous horizon, the amorphous horizon gains SOM C following a large-fire year because of substantial inputs associated with root mortality, uncombusted vegetation biomass, and residual fibrous SOM C that was "cascaded" into the amorphous pool following the model structure of Harden et al. (2000). This was followed by a long period of C loss from the amorphous horizon until the fibrous horizon SOM C built up enough so that the transfer of fibrous SOM C into amorphous horizon exceeds decomposition losses. Between 1960 and 2006, the simulation estimates that the amorphous horizon of the YRB gained 38 Tg C, most of which was from additions associated with fire.

In contrast to both the fibrous and the amorphous horizons, SOM C of the mineral horizon generally decreased starting in the 1970s in association with warming soils, except for two very slight increments during and immediately after large fires (Fig. 6b). Between 1960 and 2006, the simulation estimates that the mineral horizon of the YRB lost 24 Tg C. This trend is consistent with simulated deepening of the active layer (Fig. 7a) in forests underlain by permafrost area (which occupy ~65% of the YRB), implying more available deep SOM C for decomposition. The continuous mineral horizon C loss is also related to the simulated

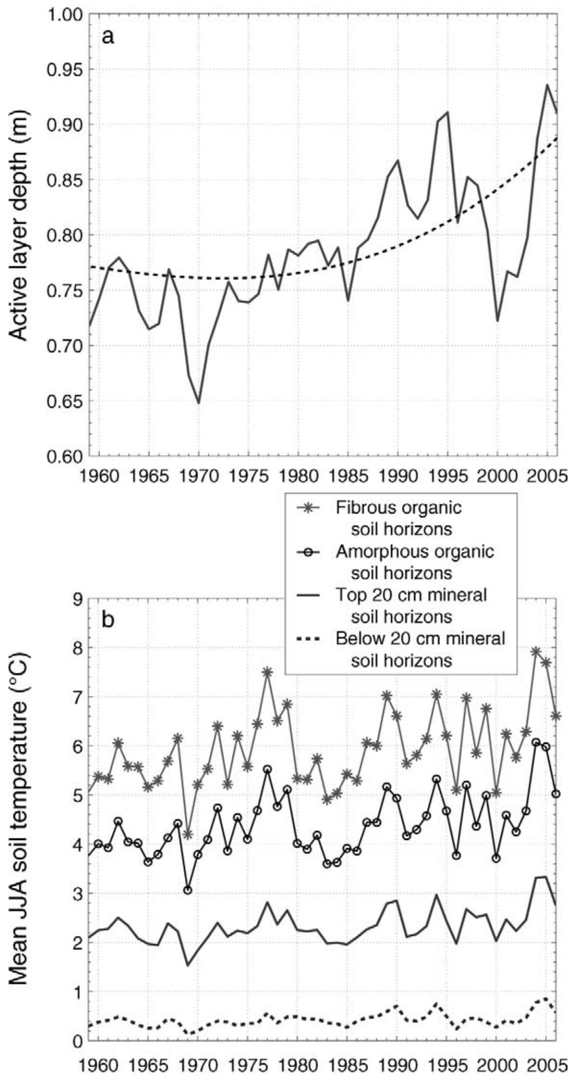

FIG. 7. (a) Mean annual active layer depth of permafrost (the solid line is the yearly active layer depth, and dashed line shows the multi-linear fitted trend line) and (b) mean June–July–August (JJA) soil temperature of four soil horizons simulated by DOS-TEM for forested portions of the Yukon River Basin from 1960 to 2006.

warming of mineral soil horizons since the mid-1970s (Fig. 7b) because C inputs were very limited.

Controls of warming and fire on subbasin C stock changes

We analyzed simulated changes in C storage for the 13 subbasins in the YRB with respect to variation in mean annual temperature (MAT) change and fractional area burned in each subbasin to evaluate the relative importance of warming and fire on spatial variability in simulated C storage. Across the subbasins, there was substantial variation in simulated changes (1960–2006) in vegetation C (+30 to −15 g $C{\cdot}m^{-2}{\cdot}yr^{-1}$) and total SOM C (+10 to −10 g $C{\cdot}m^{-2}{\cdot}yr^{-1}$). Mean annual temperature change of the 13 subbasins was not correlated with simulated changes in forest vegetation C ($R^2 = 0.0817$, $n = 13$, $P = 0.3437$) and total SOM C ($R^2 = 0.0569$, $n = 13$, $P = 0.4324$) (Fig. 8a). In contrast, changes in vegetation C and total SOM C significantly decreased with increasing fraction of burned forest area between 1960 and 2006 across the subbasins (Fig. 8b). Forest vegetation C decreased nearly linearly ($R^2 = 0.815$, $n = 13$, $P = 0.00003$) and total SOM C stocks decreased nonlinearly according to a quadratic relationship ($R^2 = 0.684$, $n = 13$, $P = 0.003$). From these relationships, it appears that ~0.70% area burned per year within a subbasin is the point at which a subbasin switches from being a sink to a source of C. Note that 0.59% of the entire YRB burned per year between 1960 and 2006 (Table 3), which is just below the sink-source transition point.

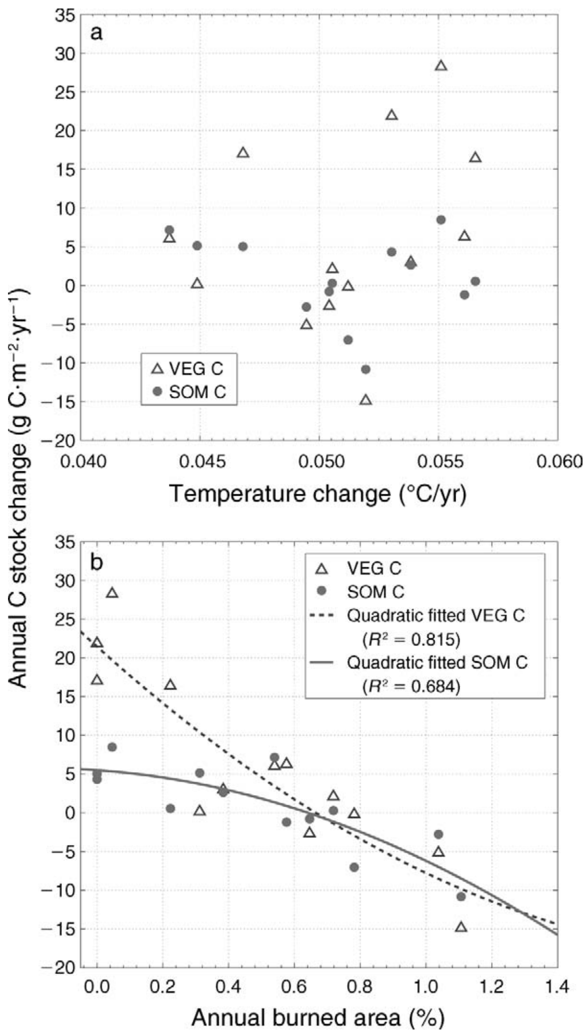

FIG. 8. Relationships of spatially averaged annual forest vegetation (VEG) and soil organic matter (SOM) C stock changes in 13 subbasins simulated by DOS-TEM from 1960 to 2006 with (a) mean annual air temperature change and (b) percentage of mean annual burned forested areas in the Yukon River Basin.

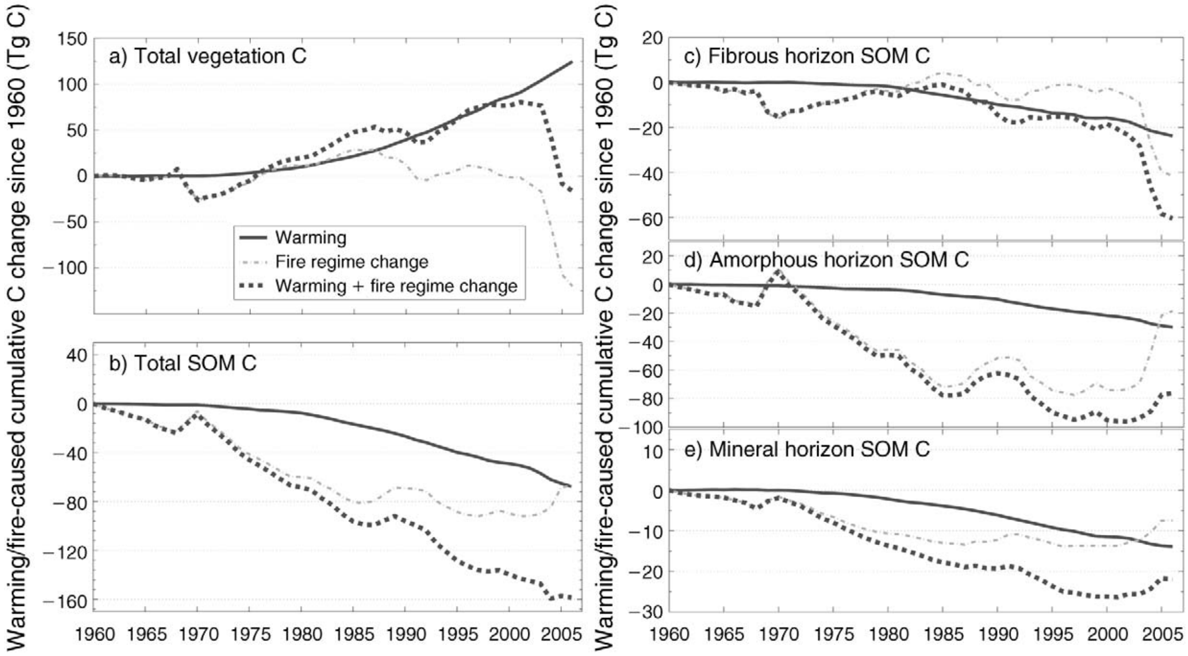

FIG. 9. The cumulative warming, fire regime change, and warming plus fire regime change effects on vegetation C and total SOM C in forests of the Yukon River Basin from 1960 to 2006 as analyzed by the DOS-TEM factorial simulation experiment conducted in this study. Note: +Warming indicates historical climate warming, −Warming indicates de-trended air temperature; +Fire indicates historical (enhancing) fire regime, −Fire indicates normalized fire regime. (1) The "Warming" effect was the difference of "+Warming and −Fire" and "−Warming and −Fire" simulations; (2) the "Fire Regime Change" effect was the difference of "−Warming and +Fire" and "−Warming and −Fire" simulations; and (3) the total "Warming + Fire Regime Change" effect were the difference of "+Warming and + Fire" and "−Warming and −Fire" simulations.

Controls of warming and changes in fire regime on whole basin C stock changes

We conducted four simulations in a factorial warming vs. fire analysis to separate the relative effects of warming and changes in fire regime on C stock changes in the YRB. The dynamics of these effects are shown in Fig. 9 and are summarized in Table 4. The warming climate gradually and steadily increased forest vegetation C stocks since the mid-1970s in comparison with the detrended air temperature ("Warming" effect in Fig. 9a) primarily because of longer growing seasons and increased nitrogen availability. In contrast, the observed fire regime did not substantially reduce forest vegetation C stocks in comparison to the normalized fire regime until the very large-fire years of the 2000s ("Fire regime change" effect in Fig. 9a). The combination of warming and changes in the fire regime generally caused

TABLE 4. Net contributions of warming and changes in fire on changes in vegetation, soil organic matter (SOM), and total C of Yukon River Basin forests from 1960 to 2006 as analyzed by the DOS-TEM factorial simulation experiment in this study.

TEM simulations	Vegetation (Tg C)	SOM (Tg C)	Total C (Tg C)
1) +Warming and +Fire	+46	+0.4	+46
2) −Warming and +Fire	−61	+92	+31
3) +Warming and −Fire	+183	+91	+274
4) −Warming and −Fire	+58	+158	+216
Total warming and change in fire regime effect (1 − 4)	−12	−158	−170
Warming effect (3 − 4)	+125	−67	+58
Change in fire regime effect (2 − 4)	−119	−66	−185
Interaction effect (total effect – warming effect – change in fire regime effect)	−18	−25	−43

Note: +Warming indicates historical climate warming, −Warming indicates de-trended air temperature; +Fire indicates historical (enhancing) fire regime, −Fire indicates normalized fire regime.

vegetation C stocks to increase in a fashion similar to that of the simulation driven by historical temperature but normalized fire regime until the very large-fire years of the 2000s ("Warming + fire regime change" effects vs. "Warming" effect in Fig. 9a). In summary the warming effect alone on forest vegetation C 1960–2006 was approximately +125 Tg C, the fire regime change effect was about −119 Tg C, and the interaction was −18 Tg C (Table 4). Based on these different model scenarios, we calculated a total warming and fire regime change effect of −12 Tg C for boreal forest ecosystems of the YRB from 1960 to 2006.

In contrast to effects on vegetation C, both warming and change in fire regime decreased SOM C stocks (Fig. 9b–e). Warming alone from 1960 to 2006 caused continuous and steady decline of SOM C in the two organic horizons and in the mineral horizon, resulting in a cumulative total SOM loss of 67 Tg C (Table 4). The effect of change in fire regime on the temporal pattern of SOM C varied among the different horizons. The changing fire regime resulted in greater losses from the fibrous horizon during big fire years, but the fibrous horizon tended to recover between large-fire years relatively quickly ("Fire regime change" in Fig. 9c), compared to in the amorphous and mineral horizon ("Fire regime change" Fig. 9d and e). Changes in the fire regime caused C in both the amorphous and mineral horizons to increase immediately after a large-fire year due to transfers of organic material from root mortality and other soil organic horizons, but these horizons subsequently lost C for several years after the large-fire years. The changing fire regime caused SOM of YRB forests to lose 66 Tg C from 1960 to 2006, which was very similar to the effect of warming on SOM C (Table 4). In summary, both warming and fire regime change resulted in 158 Tg C lower SOM than would have occurred without warming and changes in fire regime.

For the combination of vegetation and SOM C in forested areas of the YRB, warming alone increased ecosystem C stocks by 58 Tg C from 1960 to 2006, changes in the fire regime caused a loss of 185 Tg C, and the interaction of warming and changes in the fire regime resulted in an additional C loss of ~43 Tg (Table 4). The resultant loss of ecosystem C caused by warming and fire regime change was 170 Tg C (Table 4) less in comparison to a simulation without warming and with a normalized fire regime.

Discussion

In this study we validated and applied a biogeochemical model with soil organic dynamics, the DOS-TEM, to estimate changes in forest C storage between 1960 and 2006 over the YRB, which has experienced substantial warming and increases in wildfire in recent decades. Because both warming and wildfire affect terrestrial C release, this model provided us with a tool for understanding interactions among climate, disturbance, soil structure, and soil environment on ecosystem C dynamics. Here we discuss (1) how the results of this study relate to the issue of the weakening of the boreal C sink and (2) the limitations of our application of DOS-TEM. We conclude by providing thoughts on the implications of the findings of this study for mitigation efforts in support of climate policy and the application of regional biogeochemical and earth system models in assessments of carbon dynamics.

Are warming and changes in fire regime weakening the strength of the C sink in the YRB?

Our analyses with DOS-TEM indicate that forest vegetation C storage increased in the YRB by 46 Tg C between 1960 and 2006, which is 2.3 g C·m^{-2}·yr^{-1} over this time period, but that soil C storage did not change appreciably. Although there was essentially no net response of soil C storage, our analyses suggest that C has been continuously lost from the deep mineral soil horizon since warming began in about 1970. There was an increase of C in the amorphous horizon in our simulations, largely because this horizon grows from the transfer of C from the fibrous organic horizon after fire, which is consistent with field studies (Harden et al. 2000). Also, the factorial experiment we conducted indicates that warming and increases in wildfire reduced soil C storage by 158 Tg C when compared to scenario of no warming and normalized fire regime from 1960 to 2006. The effects of warming and fire contributed approximately equally to this difference, but interactions between warming and fire were responsible for 25 Tg C (16%) of the 158-Tg C reduction. This large interaction suggests that the reduction of organic horizon thickness associated with wildfire increased the vulnerability of deep-soil C stocks to warming. Much of the 158 Tg C difference was caused by the very large fires of 2004–2005 at the end of study period (1960–2006). It is important to note that soil C stocks are likely to continue to decrease for a decade or more because of warmer soils and gradually reduced C inputs to the soil. Thus, the long-term effects of the 2004–2005 fires have not been fully taken into account in our analysis.

Warming and increases in fire together reduced forest vegetation C storage by only 12 Tg C, but the effects of warming were to increase C storage by 125 Tg C and the effects of changes in fire regime were to decrease C storage by 119 Tg C. In the DOS-TEM simulations, warming tends to increase vegetation C storage because of the longer growing seasons that have been occurring in the YRB region (Euskirchen et al. 2006, Euskirchen et al. 2007), and because enhanced decomposition increases the availability of soil N to forest vegetation in which growth has been documented to be limited by the availability of N (Yarie and Van Cleve 2010). This tendency for warming to increase vegetation C storage in our simulations is only slightly offset by the combination of the effects of a changing fire regime and by the interaction between warming and changing fire regime. We interpret this interaction as the combustion of more vegetation C stocks in forests where growth has responded to warming.

Although the basin-level analyses indicate that warming and changes in fire regime are approximately equivalent in their effects on changes in forest vegetation and soil C storage, our analysis across subbasins indicates that C stock changes are primarily sensitive to the fraction of burned forest area within each subbasin. The fraction of area burned across the entire YRB between 1960 and 2006 is approximately at the sink-to-source transition point identified by the subbasin analysis. Taken together, the factorial model experiment and the subbasin analysis indicate that both warming and changes in the fire regime are weakening the C sink in the YRB, and that continued warming and more frequent fires are likely to lead to further weakening of the sink or possible reversal to a source. This is consistent with the analysis of Hayes et al. (2011).

Limitations of the application of DOS-TEM to the YRB

Several key limitations of the application of DOS-TEM to the YRB in this study include issues of model evaluation, representation of successional trajectories, representation of disturbance legacies, and specification of burn severity. Our approach to the model evaluation was to compare the site-specific application of DOS-TEM parameterizations with observed forest biomass and organic horizon thickness at the CAFI sites. The simulation of forest biomass was unbiased for black spruce, slightly overestimated for white spruce, and slightly underestimated for deciduous forests. In contrast, there was much more scatter in simulating soil organic horizon thickness at the CAFI sites, and there seemed to be a set of sites for which there was little bias and a set of sites in which DOS-TEM estimated soil organic horizon thickness that was ~50% of observed thickness. We do not have information on disturbance history for the CAFI sites, so it is not clear if the underestimation of soil organic horizon thickness is associated with the way the model was applied to the sites, or is indicative of measurement biases, or represents one or more fundamental factors not considered in the model itself (e.g., the effects of slope and aspect).

We only evaluated the model at the CAFI sites dominated by a single tree species (about two-thirds of the CAFI sites). We assumed that these sites were representative of self-replacement successional dynamics, which was the way that the model was applied to represent succession after fire. Studies associated with the Bonanza Creek LTER indicate that self-replacement of black spruce primarily occurs when there is >3 cm of the organic horizon remaining after fire, but that deciduous forest successional trajectories are possible if <3 cm remains (Johnstone et al. 2010). It has been estimated that fires in the 2000s may have reduced the area of black spruce stands by 4.2% and increased the area of deciduous forest stands by 20% in interior Alaska because of the burning of soil organic horizons in black spruce stands to <3 cm (Barrett et al. 2011). In comparison to successional trajectories involving black spruce, we have much less understanding of alternative successional trajectories for burned white spruce and deciduous forest stands; these alternative trajectories are currently being studied by Bonanza Creek LTER researchers. Ongoing model development is presently being focused on the interactions among burn severity of the soil organic horizon and successional trajectories in black spruce stands of interior Alaska, and will be directed to represent other trajectories as they become better understood.

In our application of DOS-TEM to the YRB, we used a backcasting methodology prior to the start of the historically recorded fires (1950s in Alaska, and 1960 in Canada). This uncertainty in representing fire history affects the simulated stand age distribution and the distribution of soil organic horizon thickness across the landscape of the YRB. We did not have good information on stand age distribution because ongoing U.S. and Canadian inventories do not extend into the YRB. Furthermore, severe insect disturbance of forests in interior Alaska affects an area similar to that of fire on average (McGuire et al. 2007), and is not represented in the regional simulations of DOS-TEM. Insect infestation has the potential to substantially affect regional C storage (Kurz and Apps 1999, Kurz et al. 2008). If the area being affected by insect infestation is increasing in the YRB in response to climate change as in other regions of the boreal forest in North America (e.g., see Hogg et al. 2002), we would expect the C sink in the YRB to be weakened more than what has been estimated in this study.

Another key limitation is the representation of burn severity, in particular with respect to how burn severity affects the thickness of soil organic horizons. Both the combustion of aboveground vegetation C and the depth of burning in the soil organic horizons are based on a table involving fire season, area burned in interior Alaska since the 1950s, and soil drainage type (Yi et al. 2010). More sophisticated models of burn severity have recently been developed for black spruce forest in interior Alaska (e.g., Barrett et al. 2010, 2011), and these models have the potential to drive fire severity based on topography, spectral information, spatial characteristics of a fire, and fire characteristics. An important next step in our modeling efforts is to modify the FEM of DOS-TEM to implement a more sophisticated burn severity approach.

CONCLUSION

The changes in the strength of boreal forest CO_2 sinks suggested by this analysis have implications for global carbon management policy. Attempts have been made to identify anthropogenic emission targets that, given the current rates of sequestration in terrestrial ecosystems, would result in atmospheric CO_2 concentrations stabilized at levels that mitigate the effects of future climate change. Our analysis for the YRB suggests that climate warming and associated changes in fire regime resulted in no appreciable change in soil C storage between 1960 and 2006, but that soil C storage would have increased 158 Tg C in the absence of climate warming and changes in fire regime. Such reductions in the CO_2 sink capacity of boreal forests in response to climate warming and associated changes in disturbance regime are important to take into account by international mitigation efforts focused on controlling the buildup of anthropogenic CO_2 in the atmosphere, as this loss of sink capacity could weaken and negate mitigation efforts.

The results of our study also have implications for the structure of models used to assess responses of boreal forest C to projections of future climate change. Several recent regional studies have identified that permafrost thaw is important to consider in representing the response of soil C dynamics in northern high-latitude ecosystems to ongoing and projected climate change (Zhuang et al. 2006, Hayes et al. 2011, Schaefer et al. 2011, Schneider von Deimling et al. 2012). These studies indicate that it is important to consider the depth distribution of soil C and how permafrost thaw might expose soil C to decomposition in a warming climate. Furthermore, modeling studies have also identified that soil C storage in boreal forest ecosystems is vulnerable to fire associated with ongoing and projected climate change (Balshi et al. 2009, Zhuang et al. 2006, Metsaranta et al. 2010, Hayes et al. 2011). Because C dynamics of boreal forest ecosystems have substantial implications for efforts to mitigate the growth of atmospheric CO_2 (McGuire et al. 2009), it will be important for large-scale biochemical models and earth system models to consider how warming and changes in fire regime will influence these dynamics. This study further identifies that it is important to represent the dynamics of organic soil horizons in applications of these models to assess historical changes in regional C dynamics to changes in climate and fire regime.

Acknowledgments

S.-H. Yi received support for this study through grants as part of the National Basic Research Program (2010CB951402) and One Hundred People Plan of the Chinese Academy of Sciences. Support for F.-M. Yuan, A. D. McGuire, and others in this study include the USDA (CSREES grant 2008-35615-18959), the Alaska Integrated Ecosystem Model Project (funded jointly by the U.S. Geological Survey and U.S. Fish and Wildlife Service), the Strategic Environmental Research and Defense Program of the Department of Defense, and the Bonanza Creek Long-Term Ecological Research Program (funded jointly by the National Science Foundation and the USDA Forest Service through the Pacific Northwest Research Station. E. S. Kasischke was supported through NASA grants (NNG04GD25G and NNX08AI79G).

Literature Cited

Balshi, M. S., A. D. McGuire, P. Duffy, M. Flannigan, D. W. Kicklighter, and J. Melillo. 2009. Vulnerability of carbon storage in North American boreal forests to wildfires during the 21st century. Global Change Biology 15:1491–1510.

Balshi, M. S., et al. 2007. The role of historical fire disturbance in the carbon dynamics of the pan-boreal region: A process-based analysis. Journal of Geophysical Research-Biogeosciences 112:18.

Barrett, K., E. S. Kasischke, A. D. McGuire, M. R. Turetsky, and E. S. Kane. 2010. Modeling fire severity in black spruce stands in the Alaskan boreal forest using spectral and non-spectral geospatial data. Remote Sensing of Environment 114:1494–1503.

Barrett, K., A. McGuire, E. Hoy, and E. Kasischke. 2011. Potential shifts in dominant forest cover in interior Alaska driven by variations in fire severity. Ecological Applications 21:2380–2396.

Bond-Lamberty, B., and S. T. Gower. 2007. Estimation of stand-level leaf area for boreal bryophytes. Oecologia 151:584–592.

Calef, M. P., A. D. McGuire, H. E. Epstein, T. S. Rupp, and H. H. Shugart. 2005. Analysis of vegetation distribution in Interior Alaska and sensitivity to climate change using a logistic regression approach. Journal of Biogeography 32:863–878.

Canadell, J. G., P. Ciais, K. Gurney, C. Le Quere, S. Piao, and C. L. Sabine. 2011. An international effort to quantify regional carbon fluxes. Eos 92:81–82.

Canadell, J. G., C. Le Quere, M. R. Raupach, C. B. Field, E. T. Buitenhuis, P. Ciais, T. J. Conway, N. P. Gillett, R. A. Houghton, and G. Marland. 2007*a*. Contributions to accelerating atmospheric CO_2 growth from economic activity, carbon intensity, and efficiency of natural sinks. Proceedings of the National Academy of Sciences USA 104:18866–18870.

Canadell, J. G., D. E. Pataki, R. Gifford, R. A. Houghton, Y. Luo, M. R. Raupach, P. Smith, and W. Steffen. 2007*b*. Saturation of the terrestrial carbon sink. Pages 59–78 *in* J. G. Canadell, D. E. Pataki, and L. F. Pitelka, editors. Terrestrial ecosystems in a changing world. Springer, Berlin, Germany.

Euskirchen, E. S., A. D. McGuire, and F. S. Chapin, III. 2007. Energy feedbacks of northern high-latitude ecosystems to the climate system due to reduced snow cover during 20th century warming. Global Change Biology 13:2425–2438.

Euskirchen, E. S., A. D. McGuire, D. W. Kicklighter, Q. Zhuang, J. S. Clein, R. J. Dargaville, D. G. Dye, J. S. Kimball, K. C. McDonald, J. M. Melillo, V. E. Romanovsky, and N. V. Smith. 2006. Importance of recent shifts in soil thermal dynamics on growing season length, productivity, and carbon sequestration in terrestrial high-latitude ecosystems. Global Change Biology 12:731–750.

French, N. H. F., E. S. Kasischke, and D. G. Williams. 2002. Variability in the emission of carbon-based trace gases from wildfire in the Alaskan boreal forest. Journal of Geophysical Research-Atmospheres 108:8151.

Harden, J. W., J. C. Neff, D. V. Sandberg, M. R. Turetsky, R. Ottmar, G. Gleixner, T. L. Fries, and K. L. Manies. 2004. Chemistry of burning the forest floor during the FROSTFIRE experimental burn, interior Alaska, 1999. Global Biogeochemical Cycles 18:GB3034.

Harden, J. W., E. T. Sundquist, R. F. Stallard, and R. K. Mark. 1992. Dynamics of soil carbon during deglaciation of the Laurentide Ice Sheet. Science 258:1921–1924.

Harden, J. W., S. E. Trumbore, B. J. Stocks, A. Hirsch, S. T. Gower, K. P. O'Neill, and E. S. Kasischke. 2000. The role of fire in the boreal carbon budget. Global Change Biology 6:174–184.

Hayes, D. J., A. D. McGuire, D. W. Kicklighter, K. R. Gurney, T. J. Burnside, and J. M. Melillo. 2011. Is the northern high-latitude land-based CO_2 sink weakening? Global Biogeochemical Cycles 25:GB3018.

Hogg, E. H., J. P. Brandt, and B. Kochtubajda. 2002. Growth and dieback of aspen forests in northwestern Alberta, Canada, in relation to climate and insects. Canadian Journal of Forest Research 32:823–832.

Jenkinson, D. S., and J. H. Rayner. 1977. The turnover of soil organic matter in some of the Rothamsted classical experiments. Soil Science 123:298–305.

Johnson, K. D., et al. 2011. Soil carbon distribution in Alaska in relation to soil-forming factors. Geoderma 167–168:71–84.

Johnstone, J. F., F. S. Chapin, III, T. N. Hollingsworth, M. C. Mack, V. Romanovsky, and M. Turetsky. 2010. Fire, climate change, and forest resilience in interior Alaska. Canadian Journal of Forest Research 40:1302–1312.

Jorgenson, M. T., V. Romanovsky, J. Harden, Y. Shur, J. O'Donnell, E. A. G. Schuur, M. Kanevskiy, and S. Marchenko. 2010. Resilience and vulnerability of permafrost to climate change. Canadian Journal of Forest Research 40:1219–1236.

Kasischke, E. S., and M. R. Turetsky. 2006. Recent changes in the fire regime across the North American boreal region: spatial and temporal patterns of burning across Canada and Alaska. Geophysical Research Letters 33:L13703.

Kasischke, E. S., D. Verbyla, T. S. Rupp, A. D. McGuire, K. A. Murphy, J. L. Allen, E. E. Hoy, R. Jandt, P. Duffy, M. Calef, and M. R. Turetsky. 2010. Alaska's changing fire regime: Implications for the vulnerability of its boreal forests. Canadian Journal of Forest Research 40:1313–1324.

Kasischke, E. S., D. Williams, and D. Barry. 2002. Analysis of the patterns of large fires in the boreal forest region of Alaska. International Journal of Wildland Fire 11:131–144.

Kurz, W. A., and M. J. Apps. 1999. A 70-year retrospective analysis of carbon fluxes in the Canadian forest sector. Ecological Applications 9:526–547.

Kurz, W. A., C. C. Dymond, G. Stinson, G. J. Rampley, E. T. Neilson, A. L. Carroll, T. Ebata, and L. Safranyik. 2008. Mountain pine beetle and forest carbon feedback to climate change. Nature 452:987–990.

Le Quere, C., et al. 2009. Trends in the sources and sinks of carbon dioxide. Nature Geoscience 2:831–836.

Malone, T., J. Liang, and E. C. Packee. 2009. Cooperative Alaska forest inventory. USDA Forest Sevice, Pacific Northwest Research Station, Portland, Oregon. USA.

Manies, K. L., J. W. Harden, B. P. Bond-Lamberty, and K. P. O'Neill. 2005. Woody debris along an upland chronosequence in boreal Manitoba and its impact on long-term carbon storage. Canadian Journal of Forest Research 35:472–482.

McGuire, A. D., L. G. Anderson, T. R. Christensen, S. Dallimore, L. D. Guo, D. J. Hayes, M. Heimann, T. D. Lorenson, R. W. Macdonald, and N. Roulet. 2009. Sensitivity of the carbon cycle in the Arctic to climate change. Ecological Monographs 79:523–555.

McGuire, A. D., D. J. Hayes, D. W. Kicklighter, M. Manizza, Q. Zhuang, M. Chen, M. J. Follows, K. R. Gurney, J. W. McClelland, J. M. Melillo, B. J. Peterson, and R. G. Prinn. 2010*a*. An analysis of the carbon balance of the Arctic Basin from 1997 to 2006. Tellus B 62:455–474.

McGuire, A. D., et al. 2007. Responses of high-latitude ecosystems to global change: potential consequences for the climate system. Pages 297–310 *in* J. G. Canadell, D. E. Pataki, and L. F. Pitelka, editors. Terrestrial ecosystems in a changing world. Springer, Berlin, Germany.

McGuire, A. D., R. W. Macdonald, E. A. G. Schuur, J. W. Harden, P. Kuhry, D. J. Hayes, T. R. Christensen, and M. Heimann. 2010*b*. The carbon budget of the northern cryosphere region. Current Opinion in Environmental Sustainability 2:231–236.

Metsaranta, J. M., W. A. Kurz, E. T. Neilson, and G. Stinson. 2010. Implications of future disturbance regimes on the C balance of Canada's managed forest (2010–2100). Tellus 62:719–728.

O'Donnell, J. A., V. E. Romanovsky, J. W. Harden, and A. D. McGuire. 2009*a*. The effect of moisture content on the thermal conductivity of moss and organic soil horizons from black spruce ecosystems in interior Alaska. Soil Science 174:646–651.

O'Donnell, J. A., M. R. Turetsky, J. W. Harden, K. L. Manies, L. E. Pruett, G. Shetler, and J. C. Neff. 2009*b*. Interactive effects of fire, soil climate, and moss on CO_2 fluxes in black spruce ecosystems of interior Alaska. Ecosystems 12:57–72.

Pan, Y., et al. 2011. A large and persistent carbon sink in the world's forests. Science 333:988–993.

Ruess, R. W., K. Van Cleve, J. Yarie, and L. A. Viereck. 1996. Contributions of fine root production and turnover to the carbon and nitrogen cycling in taiga forests of the Alaskan interior. Canadian Journal of Forest Research 26:1326–1336.

Schaefer, K., T. Zhang, L. Bruhwiler, and A. P. Barrett. 2011. Amount and timing of permafrost carbon release in response to climate warming. Tellus B 63:165–180.

Schneider von Deimling, T., M. Meinshausen, A. Levermann, V. Huber, K. Frieler, D. M. Lawrence, and V. Brovkin. 2012. Estimating the permafrost carbon feedback on global warming. Biogeosciences 9:649–665.

Stinson, G., W. A. Kurz, C. E. Smyth, E. T. Neilson, C. C. Dymond, J. M. Metsaranta, C. Boisvenue, G. J. Rampley, Q. Li, T. M. White, and D. Blain. 2011. An inventory-based analysis of Canada's managed forest carbon dynamics, 1990 to 2008. Global Change Biology 17:2227–2244.

Tarnocai, C., J. G. Canadell, E. A. G. Schuur, P. Kuhry, G. Mazhitova, and S. Zimov. 2009. Soil organic carbon pools in the northern circumpolar permafrost region. Global Biogeochemical Cycles 23:GB2023.

Turetsky, M. R., E. S. Kane, J. W. Harden, R. D. Ottmar, K. L. Manies, E. Hoy, and E. S. Kasischke. 2011. Recent acceleration of biomass burning and carbon losses in Alaskan forests and peatlands. Nature Geosciences 4:27–31.

Turetsky, M. R., M. C. Mack, T. N. Hollingsworth, and J. W. Harden. 2010. The role of mosses in ecosystem succession and function in Alaska's boreal forest. Canadian Journal of Forest Research 40:1237–1264.

Vogel, J. G., D. W. Valentine, and R. W. Ruess. 2005. Soil and root respiration in mature Alaskan black spruce forests that vary in soil organic matter decomposition rates. Canadian Journal of Forest Research 35:161–174.

Wang, G. G. 1995. White spruce stie index in relation to soil, understory vegetation, and foliar nutrients. Canadian Journal of Forest Research 25:29–38.

Yarie, J., and S. Billings. 2002. Carbon balance of the taiga forest within Alaska: present and future. Canadian Journal of Forest Research 32:757–767.

Yarie, J., E. Kane, and M. Mack. 2007. Aboveground biomass equations for the trees of interior Alaska. Alaska Agricultural and Forest Experimental Station Bulletin 115. University of Alaska, Fairbanks, Alaska, USA.

Yarie, J., and K. Van Cleve. 1983. Biomass and productivity of white spruce stands in interior Alaska. Canadian Journal of Forest Research 13:767–772.

Yarie, J., and K. Van Cleve. 2010. Long-term monitoring of climatic and nutritional affects on tree growth in interior Alaska. Canadian Journal of Forest Research 40:1325–1335.

Yi, S., K. Manies, J. Harden, and A. D. McGuire. 2009*a*. Characteristics of organic soil in black spruce forests: Implications for the application of land surface and ecosystem models in cold regions. Geophysical Research Letters 36:L05501.

Yi, S., A. D. McGuire, J. Harden, E. Kasischke, K. Manies, L. Hinzman, A. Liljedahl, J. Randerson, H. Liu, V. Romanovsky, S. Marchenko, and Y. Kim. 2009*b*. Interactions between soil thermal and hydrological dynamics in the response of Alaska ecosystems to fire disturbance. Journal of Geophysical Research 114:G02015.

Yi, S. H., A. D. McGuire, E. Kasischke, J. Harden, K. Manies, M. Mack, and M. Turetsky. 2010. A dynamic organic soil biogeochemical model for simulating the effects of wildfire on soil environmental conditions and carbon dynamics of black spruce forests. Journal of Geophysical Research-Biogeosciences 115:G04015.

Yi, S., M.-K. Woo, and M. A. Arain. 2007. Impacts of peat and vegetation on permafrost degradation under climate warming. Geophysical Research Letters 34:L16504.

Yoshikawa, K., W. R. Bolton, V. E. Romanovsky, M. Fukuda, and L. D. Hinzman. 2003. Impacts of wildfire on the permafrost in the boreal forests of interior Alaska. Journal of Geophysical Research-Atmospheres 108:8148.

Zhuang, Q., A. D. McGuire, K. P. O'Neill, J. W. Harden, V. E. Romanovsky, and J. Yarie. 2002. Modeling soil thermal and carbon dynamics of a fire chronosequence in interior Alaska. Journal of Geophysical Research-Atmospheres 108:8147.

Zhuang, Q. L., J. M. Melillo, M. C. Sarofim, D. W. Kicklighter, A. D. McGuire, B. S. Felzer, A. Sokolov, R. G. Prinn, P. A. Steudler, and S. M. Hu. 2006. CO_2 and CH_4 exchanges between land ecosystems and the atmosphere in northern high latitudes over the 21st century. Geophysical Research Letters 33:L17403.